IOPscience iopscience.iop.org

Home Search Collections Journals About Contact us My IOPscience

Room-temperature deposition and growth of Au on clean and oxygen passivated Si(111) surfaces investigated by optical second-harmonic generation

This article has been downloaded from IOPscience. Please scroll down to see the full text article.

1997 J. Phys.: Condens. Matter 9 9497

(http://iopscience.iop.org/0953-8984/9/44/006)

View the table of contents for this issue, or go to the journal homepage for more

Download details:
IP Address: 171.66.16.209
The article was downloaded on 14/05/2010 at 10:55

Please note that terms and conditions apply.

J. Phys.: Condens. Matter **9** (1997) 9497–9506. Printed in the UK PII: S0953-8984(97)84609-7

Room-temperature deposition and growth of Au on clean and oxygen passivated Si(111) surfaces investigated by optical second-harmonic generation

Kjeld Pedersen† and Per Morgen‡

† Institute of Physics, Aalborg University, Pontoppidanstraede 103, 9220 Aalborg Øst, Denmark
‡ Physics Department, Odense University, Campusvej 55, 5230 Odense M, Denmark

Received 23 May 1997, in final form 31 July 1997

Abstract. Room-temperature deposition and growth of Au on Si(111) is investigated by means of optical second-harmonic generation. The process on the clean 7×7 surface is compared under identical conditions to that of the oxygen passivated surface. Ordered Au/Si interfaces occur in both cases. For the 7×7 surface the interface ordering starts after deposition of 4 monolayers, completing the formation of a phase with some dissolved Si, after which a continuous Au film grows between the substrate and the mixed phase. Oxygen passivation causes interface ordering from a lower Au coverage and a considerably higher degree of interface order. Oscillating second-harmonic generation intensities versus coverage with periods in the 12–17 monolayer range show that quantum well states formed in the Au film are responsible for the second-harmonic signal. The annealing behaviours of the Au/Si structures are also studied, and discussed with the inclusion of photoemission results.

1. Introduction

The details of Au film growth on Si surfaces, and interface formation, continue to be of interest as a model system for metal/silicon interactions. A number of different models for room-temperature growth of Au films on Si(111)7×7 have been inferred from experiments over the years [1]. Most of them include a mixed layer about 15 Å thick between bulk Si and a pure Au film and, on top of the Au, an Si-rich skin layer [2]. More recent experiments, however, have shown that room-temperature growth at low deposition rates may form an abrupt interface between metallic Au and bulk Si [3]. It is always found that an Si-rich skin layer, about 1 monolayer (ML) thick, is formed after the evaporation of the first few MLs of Au, and persists at larger Au thickness.

During the last decade optical second-harmonic generation (SHG) has evolved as an interesting new probe of surface and interface regions [4, 5]. The technique owes its surface and interface sensitivity to the fact that electric dipole contributions to SHG only appear where the bulk centrosymmetry is broken [6]. Since light typically penetrates tenths of MLs into metals, even deeply buried metal/semiconductor interfaces are accessible. The technique cannot reveal as many details of the structure as diffraction of x-rays, but the symmetry properties of the interface region can be detected. Furthermore, it has been demonstrated how the population of interface electronic states can be probed with spectroscopic SHG [7].

The Au/Si system has previously been investigated with SHG by McGilp [8] who found clear evidence of an ordered interface structure. In the present work the film growth is

0953-8984/97/449497+10$19.50 © 1997 IOP Publishing Ltd

followed continuously during evaporation. The effect of the dangling bonds on the interface formation is investigated from film growth on both clean and oxide covered substrates. By comparison to recent SHG studies of Au on Co [9] it is found that quantum well (QW) states are formed in the film.

2. SHG from thin films

The SHG from the metal/semiconductor interface appears coherently added to contributions from the rest of the thin-film system. A theoretical modelling of the dependence on principal parameters such as film thickness and angle of incidence will therefore be useful in the attempts to isolate the interface contribution. In this section a phenomenological model of SHG from a thin metallic film on a substrate is discussed.

Several schemes for the treatment of SHG from multilayer structures have been developed [10, 11]. Techniques based on transfer matrices are useful when the sample consists of several layers. In the present case with a single layer on a substrate the formalism and notation derived by Sipe [12] will be useful. The sources of SHG to be considered are located at (i) the free surface, (ii) the bulk film, and (iii) the buried interface. At the pump frequency used in this work (1.17 eV) SHG from bulk Si can be neglected as it is shown by experiments where the surface has been exposed to oxygen [13]. As the substrate is (111) oriented it is from the start assumed that all three sources have threefold symmetry. The special case of isotropic SHG is then obtained by letting the appropriate tensor elements vanish.

Expressions for the reflected SH fields generated by each of the three sources mentioned above are given in [12]. Multiple reflections in the thin film of both the pump and the SH fields must also be taken into account [14] since they affect the overall magnitude and thickness dependence of the SH signal. The nonlinear polarizations of the three sources, expressed in terms of response tensors, can be obtained from [15]. In order to be able to discuss contributions to SHG from different tensor elements the nonlinear dipole polarization of an interface with C_{3v} symmetry is given. The components of the polarization along the unit vectors $\hat{s}$, $\hat{\kappa}$, and $\hat{z}$ are given by

$$P_s(2\omega) = \chi_{xxx}[(f_c^2 E_p^2 - E_s^2)\sin 3\phi - 2 f_c E_s E_p \cos 3\phi] + 2\chi_{xzx} f_c E_s E_p \tag{1}$$

$$P_\kappa(2\omega) = \chi_{xxx}[(f_c^2 E_p^2 - E_s^2)\cos 3\phi + 2 f_c E_s E_p \sin 3\phi] + 2\chi_{xzx} f_c f_s E_p^2 \tag{2}$$

$$P_z(2\omega) = \chi_{zxx}(f_c^2 E_p^2 + E_s^2) + \chi_{zzz} f_s^2 E_p^2 \tag{3}$$

where $\hat{s}$ and $\hat{\kappa}$ are in the plane of the surface and perpendicular and parallel to the plane of incidence, respectively, and $\hat{z}$ is perpendicular to the surface. The quantities f_s and f_c depend on the angle of incidence and linear optical properties. The polarization components in the plane of the surface vary with the angle ϕ between the plane of incidence and the x-axis which is along a $[11\bar{2}]$-direction in the crystal. The response tensor elements, χ_{zxx}, χ_{xzx}, and χ_{zzz} give isotropic contributions to SHG while χ_{xxx} gives rotational anisotropy.

The reflected s-polarized field only involves P_s while the p-polarized field contains a combination of P_κ and P_z. In the present experiments the sample was oriented with $\phi = 30^\circ$. In that case only χ_{xxx} contributes to s-polarized SHG from the interfaces when pure s- or p-polarized pump fields are used. The s to p combination depends only on χ_{zxx} while p to p polarization involves a combination of χ_{zxx}, χ_{xzx}, and χ_{zzz}. The existence of χ_{xxx} requires an ordered structure and s-polarized SHG is therefore used to monitor order in the system.

3. Experimental results and discussion

The Si samples were cut from 1 mm thick n-type P-doped wafers with a resistivity of 4.5 Ω cm. X-ray diffraction showed that the wafers were (111) oriented within $\pm 0.3^\circ$. Clean surfaces with negligible traces of impurities and sharp 7×7 LEED patterns were obtained by a direct resistive heating procedure. Gold was evaporated from a wire heated by a tungsten coil and the evaporation rate was measured by a quartz oscillator before and after deposition. During the evaporation the pressure stayed below 2×10^{-10} mbar. The SHG measurements were performed with a *Q*-switched Nd:YAG laser delivering 10 ns pulses at 20 Hz repetition rate with a wavelength of 1064 nm. The pulse energy was below 10 mJ in a 0.25 cm^2 spot to keep the temperature rise during measurements at a few degrees and thus with negligible effects on the growth process [5]. The SH signal was detected by a photomultiplier tube connected to gated electronics and was recorded continuously at 35° angle of incidence during Au evaporation.

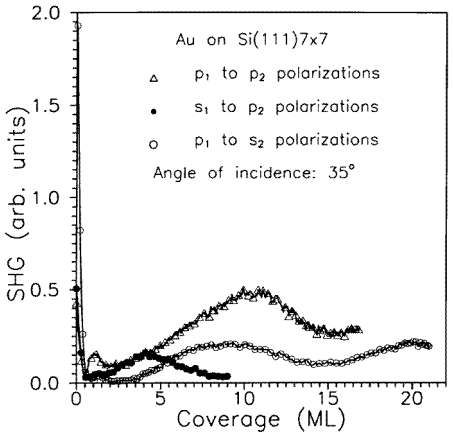

Figure 1. SHG as a function of Au coverage on Si(111)7×7 measured with three different incident and reflected light polarizations.

3.1. Initial interface formation

The variation of the SH intensity with Au coverage has been followed for three polarization combinations of pump and SH light. Figure 1 shows the results for p to p, p to s, and s to p polarizations obtained with the bare 7×7 surface as substrate. Initially, the SH signals decay fast upon Au evaporation for all three polarization configurations. It is expected that the relatively loosely bound Si adatoms are the first to be removed by the adsorbate. This is consistent with observations made by LEED where it was found that the sharpness of the 7×7 structure decayed quickly during evaporation of the first ML. At 3 ML it was still possible to see traces of the 7×7 reconstruction but no LEED pattern could be observed for coverages above 5 ML. In the same coverage range, the width of the Si(LLV) Auger peak gradually increased, ending as the well known double peak ascribed to mixed Au and Si at the surface [16]. The composition has been reported to be about three Au atoms for each Si atom [3]. With the loss of the adatoms the associated dangling-bond surface states disappear. These states are responsible for the large resonant SH signal generated by 1064 nm pump light on the 7×7 surface [17–19] and, consequently, this signal disappears.

In the range from 2 to 4 ML the order of the system is rather low as it is seen from the p to s signal of figure 1. The s to p signal on the other hand attains a maximum in this coverage range. This signal, represented by the χ_{zxx} tensor element, describes a nonlinear polarization normal to the surface generated by a pump field along the surface. SHG in this configuration requires coupling of charge movements parallel and perpendicular to the surface. In the absence of resonances this coupling is found to be weak for a microscopically flat surface with full translational symmetry along the surface. Enhancement of this coupling is observed for the 7×7 surface where transitions between occupied and empty dangling bond sites displaced both parallel and perpendicular to the surface are resonantly excited [20]. In that case removal of adatoms by oxygen exposure reduces the s to p signal by almost two orders of magnitude. Also metal islands can couple charge oscillations along the surface to oscillations normal to the surface. This could explain a peak in this signal at 4 ML. The presence of islands in this coverage range is supported by observations of traces of a 7×7 LEED-pattern at 3 ML coverage and directly indicated from x-ray photoelectron spectroscopy and x-ray stimulated AES studies [21].

At 4 ML coverage all three curves in figure 1 show characteristic structures. The p to s signal starts to increase, the s to p signal has a maximum, and the growth of the p to p signal has a change of slope. This can be compared to recent results obtained by synchrotron radiation photoemission spectroscopy studies [3] of the Si 2p and Au 4f spectra at different photon energies. It was found that the growth of the reacted Si 2p peak saturates at 4 ML. At higher coverages a continuous Au layer grows underneath the mixed Au–Si layer with an abrupt Au/Si interface. In the present experiments no LEED pattern was detected for coverages above 5 ML. The increasing order observed by SHG must therefore be for the Au/Si interface. The onset of ordering coincides with the coverage where Yeh *et al* [3] and Morgen *et al* [21] found the beginning of growth of a continuous Au layer. This also agrees with the decrease in the s to p signal, the combination previously attributed to islands.

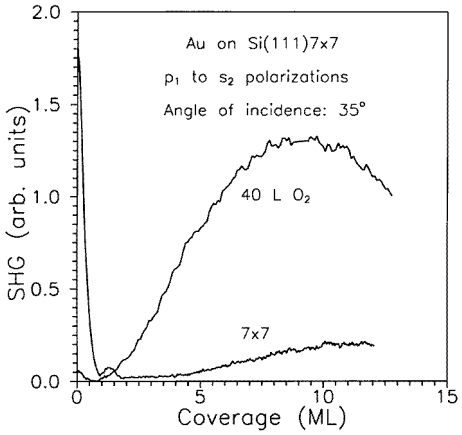

Figure 2. Comparison of SHG versus Au coverage for clean and oxygen exposed Si(111)7×7 surfaces.

Modifications of the substrate surface are expected to affect the thin-film growth process. A prominent feature of the 7×7 surface is the presence of adatoms and dangling bonds which makes this surface very reactive. Adsorption of hydrogen and oxygen are well known techniques for passivation of these bonds. The effect of a thin surface oxide on the growth mode of an Au film is illustrated by the results in figure 2. Results for the three different

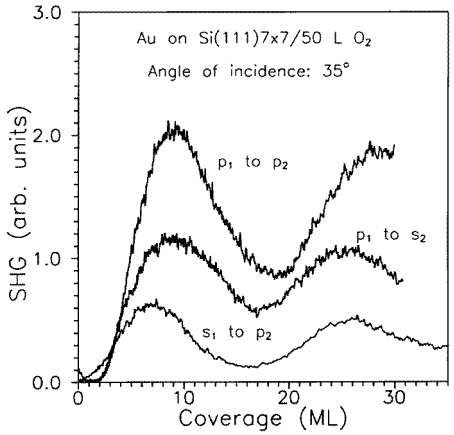

Figure 3. SHG as a function of Au coverage on Si(111)7 × 7 exposed to 50 L O_2 prior to Au evaporation. The signals were recorded with three different combinations of incident and detected light polarizations.

polarization configurations over a larger coverage scale are shown in figure 3. Prior to Au evaporation the 7×7 surface was exposed to 50 Langmuir (L) O_2 at room temperature. This leads to the formation of one ML of surface oxide, rendering the surface inert to further oxygen uptake. As the oxygen adsorption removes the dangling bonds, the SH signals associated with all three polarization combinations nearly vanish as has been discussed in a number of works [13, 18, 19].

Oxygen on the 7×7 surface clearly has a dramatic effect on the Au film growth process. For the clean 7×7 surface the delayed onset of ordering of the interface is due to the dissolution of some Si in the process of establishing the first few Au layers. When the substrate is covered by a monolayer of surface oxide the dissolution of Si is hindered. However, even in this case the Si(LVV) AES peak of the surface broadens into a double peak, but the peak height (relative to the Au(NVV) peak) is only about half of that found for Au on the 7×7 surface. Oxygen passivation thus leads to less Si in the mixed layer at the top surface before the formation of a continuous Au layer starts. Ordering of the Au/Si interface therefore also starts at a lower coverage.

Room-temperature exposure of the 7×7 surface to O_2 leads to insertion of oxygen atoms between the first and second layers of the surface [22] and, as seen by LEED, also to loss of long-range order of the surface. It may therefore at first sight seem surprising that Au deposition on this surface should give a well ordered interface. However, LEED [22, 23] has shown that patches of the oxygenated surface exist in the 7×7 structure, even after thousands of L O_2 exposure. At the same time Au adsorption is significantly less disruptive with respect to the oxygenated surface, judged from the lowered number of Si atoms on top of the Au layers in this case. With these observations in mind, it seems plausible that the resulting Au/Si interface, even without annealing, could have a better short-range order along the surface, and affect a smaller number of layers perpendicular to the interface, compared with the clean 7×7 surface.

The expressions for the nonlinear polarizations in (1) to (3) are derived for an interface with C_{3v} symmetry. It is therefore important to check whether the system still has threefold symmetry after Au deposition. At normal incidence the rotational anisotropy is detected by combined rotation of the polarization directions of the pump and SH light. In figure 4 the

rotational anisotropy of an oxygenated surface covered by 10 ML Au is compared to that of the clean 7×7 substrate. Both surfaces show threefold symmetry. The same holds when the Au film is grown on the clean 7×7 substrate [24].

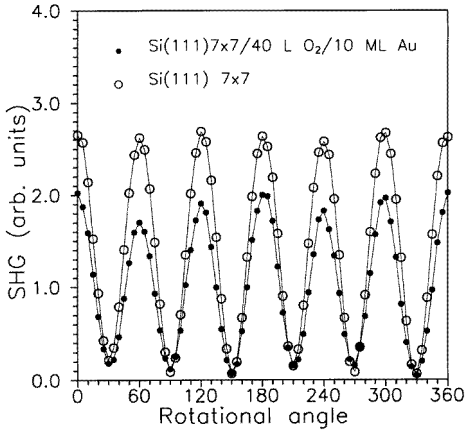

Figure 4. Rotational anisotropy of SHG from an oxide passivated Si(111)7×7 surface covered by 10 ML Au compared to that of a clean 7×7 surface.

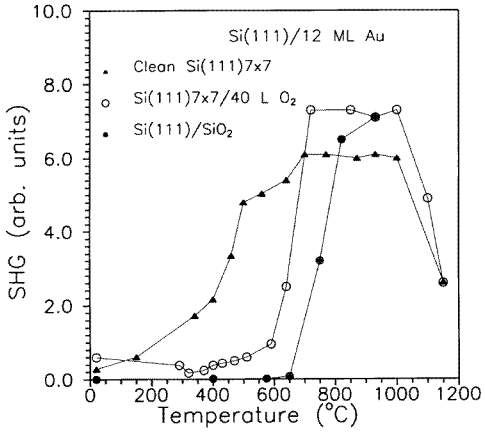

Figure 5. Comparison of SHG as a function of annealing temperature for three different Si(111) substrates covered by thin Au films.

3.2. Annealing of deposited films

Information about the thermal properties of the buried interface is also obtained from SHG, LEED, and photoemission experiments carried out during annealing of the Au films. Figure 5 shows the variation in the p to s polarized SHG as a function of annealing temperature of Au films on different substrates. The temperatures were stabilized at the values shown in the plots before the sample was allowed to cool down to room temperature and SHG was recorded. The straight lines connecting points are guides to the eye only. All systems in this plot have a Au coverage of about 30 Å. The reactions proceed with striking

differences between the clean and oxygenated surfaces. On the clean 7×7 surface, the interface structure undergoes a gradual change up to 400 °C, then shows another gradual change up to 700 °C, after which no changes are observed up to 1000 °C. Above 1000 °C a rather steep change is observed. From LEED observations of this system it is concluded that during the first phase no LEED pattern is visible, probably due to the thickness of the Au layer. A $(\sqrt{3} \times \sqrt{3})R30°$ pattern is visible above 400 °C, and becomes very sharp after annealing at subsequently higher temperatures, until it is changed into a high-quality 7×7 pattern at the end of the cycle, where the temperature is increased to above 1000 °C.

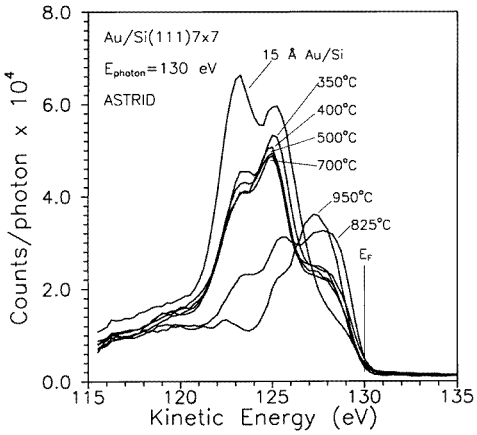

Figure 6. Photoemission of a 15 Å Au film on Si(111) after various annealing cycles to the temperatures indicated on the figure recorded with a photon energy of 130 eV.

Figure 6 shows photoemission results for an initial Au thickness of 15 Å deposited on a clean 7×7 surface. The surface composition of the sample, monitored through the valence band distribution, changes from completely Au-like to clean Si with the treatments. Significant changes appear upon heating the sample to 350 °C, or just around the eutectic temperature of the 3D Au–Si system. Progressive heatings to higher temperatures reduce the Au concentration and the clean Si spectrum is obtained after heating to 950 °C.

For the 7×7 structure the formation of the $(\sqrt{3} \times \sqrt{3})R30°$ starts at about 400 °C while it is delayed to 600 °C for the oxygen passivated surface. These results strongly indicate that the oxygen is present at the interface below the Au film and that this effectively establishes a barrier for Au diffusion into Si. An even higher barrier is obtained by 20 Å SiO_2 where the Au diffusion starts when the SiO_2 layer breaks up above 700 °C. At the same time, the Au film is then completely disordered before it has been annealed above 700 °C.

3.3. Signal oscillations with coverage

Deposition on both the clean and the oxygenated sample leads to oscillating SHG with coverage for all three polarization combinations. The period is 12 ML for the clean 7×7 substrate and 17 ML for the oxygenated substrate. Effects of optical interference between different sources combined with multiple reflections in the film can be evaluated using the model described in section 2. Numerical estimations of the values of the isotropic response tensors can be obtained from different microscopic models. The bulk polarizability γ of the Au film can be represented by the free-electron result [25] using experimental values for the linear optical properties [14]. Still following the free-electron theory, it is assumed for both

interfaces that $\chi_{zxx} = 0$ and $\chi_{xzx} = -2b\gamma$ with $b = -1$. The polarizability perpendicular to the interfaces is given by $\chi_{zzz} = -2a\gamma$ where the value $a = -17 - \mathrm{i}4$ obtained by Liebsch and Shaich [26] is used for the free surface and $a = -11$ calculated by Krijn and Geurts [27] is used to represent the Au/Si contact.

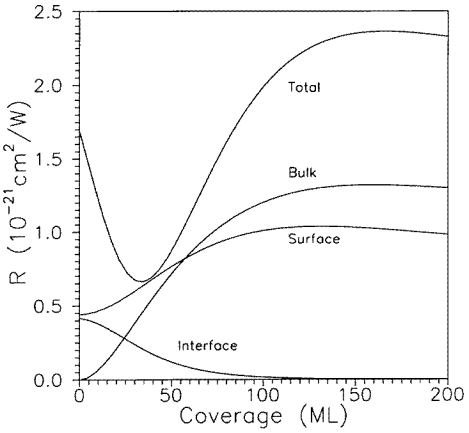

Figure 7. The isotropic part of the SHG reflectivity as a function of film thickness calculated for 35° angle of incidence. The total signal is shown together with the contributions from the free surface, the buried interface, and from the bulk film.

Figure 7 shows the thickness dependence of the total SH reflectivity together with the individual contributions calculated with the parameters described above. The bulk contribution grows monotonically as the interaction volume increases during the formation of the first 100 ML. In the same range the interface contribution decays due to absorption of the optical fields in the film. The variations in the surface contribution are due to optical interference effects in the Au film. In the calculations leading to figure 7 it is assumed that the two interface contributions are present from the start of the film growth. However, as discussed above it takes deposition of a few MLs before a continuous Au film and thus the interfaces are formed. The SH signals will therefore initially grow due to the formation of the interfaces before they follow the decay with coverage seen in figure 7. Though this might explain the first maximum at about 10 ML, the following variations of SHG with coverage in figures 1 to 3 are an order of magnitude faster than those calculated for optical interference effects. Thus, in order to model the oscillations in SHG the nonlinear response tensors must vary with film thickness.

Oscillating SHG with film thickness has previously been observed and discussed [9, 28] for Au and Cu epitaxial films on Co. For the Au film the period was found to be 13 ML and 16 ML for p to p and s to p polarizations, respectively. Within our experimental uncertainty, estimated to be ± 3 ML, the periods in the present experiments are identical to those of [9]. It is thus very likely that the oscillations have the same origin in the two sets of experiments.

Kirilyuk *et al* [9] found that the oscillations are caused by QW states in the metal film. They showed that the nonlinear susceptibility of each of the two film interfaces oscillates with a period of 7 ML in agreement with linear magnetooptical experiments. This period was taken as a measure of the local density of states at the interfaces. The slower variation with the double period in SHG experiments is a result of coherent addition of the two interface contributions with appropriate phases. Furthermore, it was found that the contribution from the bulk Au film is small compared to the interface contributions.

Despite the lack of a microscopic analysis of the oscillations, some information about the growth mode can be deduced. The mere presence of oscillations shows that the growth mode must be closely approaching layer by layer growth. Formation of islands several MLs thick would smear out the oscillations.

From their photoemission experiments Yeh *et al* [3] concluded that the Au/Si interface is abrupt while the present experiments show, in addition, that the interface is ordered. The present SHG experiments for Au on the clean substrate support the conclusions of Yeh *et al* since it is difficult to understand the behaviour of the p to s signal unless the interface is relatively sharp. The ordering sets in at 4 ML where the p to s signal starts to increase towards the first maximum at 10 ML and the next maximum is reached after additionally 12 MLs of Au. Thus, the growth of the SH signal from zero at 4 ML to its first maximum takes place at precisely half an oscillation period. The formation of QW states therefore starts at 4 ML. This does not leave much room for any diffuse, intermixed Au/Si zone as inferred from some of the early experiments on this system [2].

In addition to higher maximum levels of the signals the oxygen passivation also leads to higher oscillation amplitudes. This is explained by sharper QW interfaces on the oxygen passivated substrates where the mixed Au/Si layer at the free surface is thinner and the interface to Si is better ordered. Annealing of the film (figure 5) grown on the clean substrate leads to increasing order, also at temperatures below the onset of dissolution of Au in bulk Si (figure 6). In contrast, the film on the oxygenated substrate shows no increase in order before it is annealed above the temperature where the interface oxide breaks up. This indicates a relatively well ordered interface of the film at room temperature. Furthermore, the maximum p to s signal of the film on the oxygenated surface in figure 2 is already comparable to the resonant signal of the clean 7×7 surface. The origin of the even higher signal of the $(\sqrt{3} \times \sqrt{3})R30^\circ$ structure has not yet been investigated.

As previously discussed the p to s polarization combination only gives SHG from an ordered system. Investigations with LEED show that the free surface is disordered. Nevertheless, the modulation depth of the oscillations in the p to s signal in figure 3 is almost as strong as for the isotropic signals. According to the model in [9] one would then expect two ordered interfaces. The disorder detected by LEED may therefore be connected to the thin Si-rich skin layer while the rest of the film has a higher degree of order.

4. Conclusions

The SHG investigations show a clear dependence on substrate conditions for room-temperature growth of Au on Si. Exposing the 7×7 surface to O_2 at room temperature creates a single monolayer of surface oxide which stabilizes the surface against mixing of Au and Si. This leads to a higher degree of order at the buried interface formed upon Au growth on this passivated surface as compared to the interface with a clean 7×7 substrate. After growth of a few tens of ML of Au the oxygen is still present at the interface where it maintains a barrier for diffusion of Au and Si. An Si-rich skin layer is formed during evaporation of the first 2–4 ML of Au, again depending on substrate conditions. After formation of this layer the Au film grows with a sharp boundary to the Si substrate in a layer by layer mode, and QW states in the Au film give rise to oscillating SHG with coverage. Clearly the period and amplitude of the oscillations contain important information about the thin-film system. However, more detailed extraction of information from the data must await microscopic modelling of SHG from metallic QWs.

Acknowledgment

Both the photoemission experiments performed at the Astrid storage ring at Aarhus University and the SHG experiments were supported by the Danish Natural Science Research Council.

References

[1] Molodtsov S L, Laubschat C, Kaindl G, Shikin A M and Adamchuk V K 1991 *Phys. Rev.* B **44** 8850
[2] LeLay G 1983 *Surf. Sci.* **132** 169
[3] Yeh J-J, Hwang J, Bertness K, Friedman D J, Cao R and Lindau I 1993 *Phys. Rev. Lett.* **70** 3768
[4] McGilp J F 1995 *Prog. Surf. Sci.* **49** 1
[5] Heinz T F 1991 *Nonlinear Surface Electromagnetic Phenomena* ed H-E Ponath and G I Stegeman (Amsterdam: North-Holland) p 353
[6] Guyot-Sionnest P, Chen W and Shen Y R 1986 *Phys. Rev.* B **33** 8254
[7] Heinz T F, Himpsel F J, Palange E and Burstein E *Phys. Rev. Lett.* **63** 644
[8] McGilp J F 1987 *J. Vac. Sci. Technol.* A **5** 1442
[9] Kirilyuk A, Rasing Th, Mégy R and Beauvillain P 1996 *Phys. Rev. Lett.* **77** 4608
[10] Bethune D S 1989 *J. Opt. Soc. Am.* B **6** 910
[11] Hashizume N, Ohashi M, Kondo T and Ito R 1995 *J. Opt. Soc. Am.* B **12** 1894
[12] Sipe J E 1987 *J. Opt. Soc. Am.* B **4** 481
[13] Tom H W K and Aumiller G D 1986 *J. Opt. Soc. Am.* B **3** P184
[14] Palik E D (ed) 1985 *Handbook of Optical Constants of Solids* (Orlando, FL: Academic)
[15] Sipe J E, Moss D J and van Driel H M 1987 *Phys. Rev.* B **35** 1129
[16] Perfetti P, Nannarone S, Patella F, Quaresima C, Capozi M, Savoia A and Ottaviani G 1982 *Phys. Rev.* B **26** 1125
[17] Power J R and McGilp J F 1993 *Surf. Sci.* **287/288** 708
[18] Bratu P, Kompa K L and Höfer U 1994 *Phys. Rev.* B **49** 14 070
[19] Pedersen K and Morgen P 1995 *Phys. Rev.* B **52** R2277
[20] Pedersen K and Morgen P 1997 *Surf. Sci.* **377-379** 393
[21] Morgen P, Simonsen A C and Pedersen K 1994 *Control of Semiconductor Interfaces* ed I Ohdomari, M Oshima and A Hiraki (Amsterdam: Elsevier) pp 371–8
[22] Höfer U, Morgen P, Wurth W and Umbach E 1989 *Phys. Rev.* B **40** 1130
[23] Gipson J M 1990 *Surf. Sci.* **239** L531
[24] Pedersen K and Morgen P 1994 *Phys. Scr.* T **54** 238
[25] Sipe J E and Stegemann G I 1982 *Surface Polaritons* ed V M Agranovich and D L Mils (Amsterdam: North-Holland) p 661
[26] Liebsch A and Schaich W L 1989 *Phys. Rev.* B **40** 5401
[27] Krijn M P C and Geurts B J 1991 *Phys. Rev.* B **44** 10 712
[28] Groot Koerkamp M, Kirilyuk A, de Jong W and Rasing Th 1996 *J. Appl. Phys.* **79** 5632